Supplementary Information

TDP-43 assessment and individual staging

Assessment of TDP-43 pathology employed immunohistochemistry using a phospho-TDP-43 antibody (Cosmo Bio USA)[1], and followed a standardized regional evaluation of TDP-43-immunoreactive inclusions in the spinal cord, amygdala, hippocampus, entorhinal cortex/inferior temporal gyrus, and the frontal neocortex, as described by Katsumata et al. [2]. In the present study, presence of LATE-NC was defined based on TDP-43-immunoreactive inclusions in the amygdala, hippocampus, and/or entorhinal cortex/inferior temporal gyrus. These data were then used together with frontal neocortex TDP-43 assessments for estimating the stages reported in Table 1 as follows: 1 – TDP-43 in amygdala only; 2 – TDP-43 in hippocampus or entorhinal cortex, but not frontal neocortex; 3 – TDP-43 in frontal neocortex and any of the other regions. Note that this staging system is a slightly adapted version of the simplified staging system proposed by Nelson et al. [3]. We chose this adaptation because some autopsy cases would not have been stageable according to the originally proposed criteria. Thus, 2 cases (1 LATE-NC and 1 AD+LATE-NC) had TDP-43 in the hippocampus but not in the amygdala (1 additional LATE-NC case had missing data for the amygdala). Another 4 cases (1 LATE-NC and 3 AD+LATE-NC) had TDP-43 in the entorhinal cortex/inferior temporal gyrus and the amygdala but not in the hippocampus, and 2 cases (both AD+LATE-NC) had TDP-43 in the entorhinal cortex/inferior temporal gyrus but not in the amygdala or the hippocampus. The described adaptation of the staging system allowed staging all these cases as stage 2. Of note, all 7 cases with frontal neocortex TDP-43 also had TDP-43 in the other regions (although 2 had a negative scoring in the hippocampus), and these were thus classified as stage 3.

ADNI memory and executive function composite scores

The ADNI memory and executive function composite scores include a variety of individual tests that were selected from the extensive ADNI neuropsychological battery using initial expert ratings followed by iterative confirmatory factor analysis. The individual tests and their integration into composite scores are described in detail in the ADNI documentation and have also been published previously [4, 5]. In brief, the ADNI memory composite score included individual test items from the Rey Auditory Verbal Learning Test (RAVLT), the Logical Memory Test, as well as the memory items from the ADAS-cog and MMSE assessments. The ADNI executive function composite score included Category Fluency—animals, Category Fluency—vegetables, Trails A and B, as well as Digit span backwards, WAIS-R Digit Symbol Substitution, and 5 Clock Drawing items (circle, symbol, numbers, hands, time).

Possible neuropathologic correlates of a LATE-NC-like FDG-PET pattern

The distinct biomarker, clinical, and genetic features characterizing the amnestic dementia patients with a LATE-NC-like FDG-PET pattern in our study are consistent with an underlying LATE neuropathology and argue against typical AD pathology as the primary pathologic substrate in these patients. However, one cannot exclude that other age-related pathologies that preferentially target the medial temporal lobe, such as

primary age-related tauopathy (PART), argyrophilic grain disease (AGD), or a limbic-predominant AD subtype, may also be present in subsets of these patients, particularly because these could be assumed to associate with similar topographic FDG-PET features as the LATE-NC-typical pattern used for patient classification in our study (i.e., disproportionate medial temporal lobe hypometabolism) [6, 7]. Furthermore, these pathologies are often comorbid with LATE-NC and may interactively influence the neurodegenerative and clinical phenotype [8-10].

For example, medial temporal tau pathology required for a pathologic diagnosis of PART is nearly ubiquitous in advanced age, and additional LATE-NC associates with more pronounced medial temporal lobe atrophy in cases with PART [10, 11]. Accordingly, all the pattern-defining LATE-NC cases in our autopsy sample also exhibited some degree of medial temporal tau pathology (Braak stages I-IV) but no or only low neuritic plaques (see Table 1), thus also meeting pathologic criteria for PART [11].

In order to further explore the specificity of the FDG-PET signature to LATE-NC compared to PART, we performed an additional analysis by classifying all cases in the autopsy cohort with a B score > 0 and an A score ≤ 1 as (possible) PART. Given that this was only the case for 8 subjects, we also included cases with an A score of 2 (Thal phase 3), as long as their C score was ≤ 1 [11]. A total of 15 cases met this operational definition of PART, including the 7 cases in the LATE-NC group. Compared to healthy controls, the PART cases without LATE-NC (N=8) showed some mild hypometabolism in subcortical areas, the midcingulate, and diffuse neocortical areas, but hardly any hypometabolism in the medial temporal lobe (see supplementary Fig. S12-C below). The striking difference in medial temporal hypometabolism between PART cases with and without LATE-NC was further confirmed in a direct comparison between these two groups (Fig. S12-D), and also remained when restricting the PART cases without LATE-NC to those with cognitive impairment at last clinical evaluation (N=4; data not separately shown; no PART + LATE-NC cases were cognitively normal at last clinical evaluation). The IMT ratio was also considerably smaller in the PART cases without LATE-NC (IMT = 1.32±0.10) compared to those with LATE-NC (IMT = 1.47±0.20; d = -0.94), although this difference did not reach statistical significance in this small sample (p=0.09).

Another possible pathologic cofounder is AGD, which is also common in advanced age, often comorbid with LATE-NC, and has a similar predilection for the medial temporal lobe [12, 13]. Indeed, in our study sample, comorbid AGD was significantly more common in the LATE-NC group (5/7, 71%) compared to the AD (0%) and AD+LATE-NC (20%) groups (see Table 1 of the main manuscript). In order to explore a possible influence of this highly comorbid pathology in our LATE-NC group, we conducted a similar sensitivity analysis as described for the PART cases above. Thus, we identified a total of 10 autopsy cases in the cohort who had AGD without high ADNC, including the 5 cases in the LATE-NC group. Compared to healthy controls, the AGD cases without LATE-NC (N=5) showed a posterior cortical pattern of hypometabolism that also involved the occipital lobe, with relatively spared metabolism in the medial temporal lobe (Fig. S12-E). A direct group comparison further confirmed the striking difference in medial temporal hypometabolism between AGD cases with and without LATE-NC (Fig. S12-F). The IMT ratio was also considerably smaller in the AGD cases without LATE-NC (IMT = 1.29±0.14) compared to those with LATE-NC (IMT = 1.46±0.24; d = -0.86), although this difference did not reach statistical significance in this small sample (p=0.21). Although sample sizes are small, this data corroborates that the

distinct temporo-limbic hypometabolic pattern characterizing the LATE-NC group is indeed driven by LATE-NC rather than by comorbid PART or AGD.

On the other hand, some of the clinical features characterizing the classified LATE-NC-like patients in our study, such as older age, a memory-predominant cognitive profile, and a relatively slower disease progression, are also characteristic features of the "limbic-predominant" pathologic subtype of AD. Limbic-predominant AD is the AD subtype that is most often comorbid with LATE-NC [9, 14, 15] and it may also share some topographic features with the autopsy-derived LATE-NC-typical pattern derived here (i.e. disproportionate medial temporal lobe hypometabolism)[6, 7, 16]. However, in contrast to the classified LATE-NC-like cases in our study, the limbic-predominant AD subtype is not associated with lower levels of amyloid or tau pathology [6, 15]. Moreover, in contrast to LATE-NC, the limbic-predominant AD subtype is not associated with the *TMEM106B* risk allele, and it is actually associated with the highest *APOE4* frequency across AD subtypes [8, 15]. Hence, these data argue against the possibility that the dementia patients classified as LATE-NC-like in our study may merely reflect a limbic-predominant AD subtype. However, more research is necessary to better understand interactions between LATE-NC and the limbic-predominant presentation of AD, and how neuroimaging or other biomarkers may be used to optimally differentiate between these underlying pathologies.

Supplementary Figure S1. Flow chart of inclusion/exclusion criteria for the studied autopsy sample

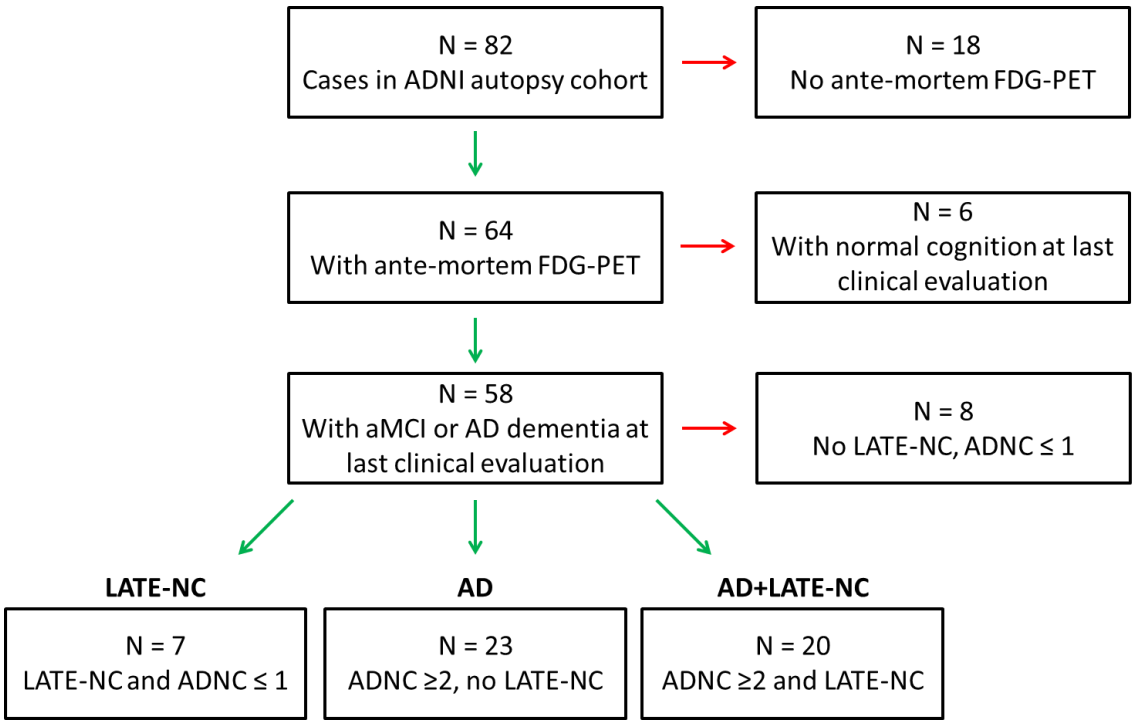

Supplementary Figure S2. Classification of individual FDG-PET scans based on spatial correlation with pathology-specific patterns

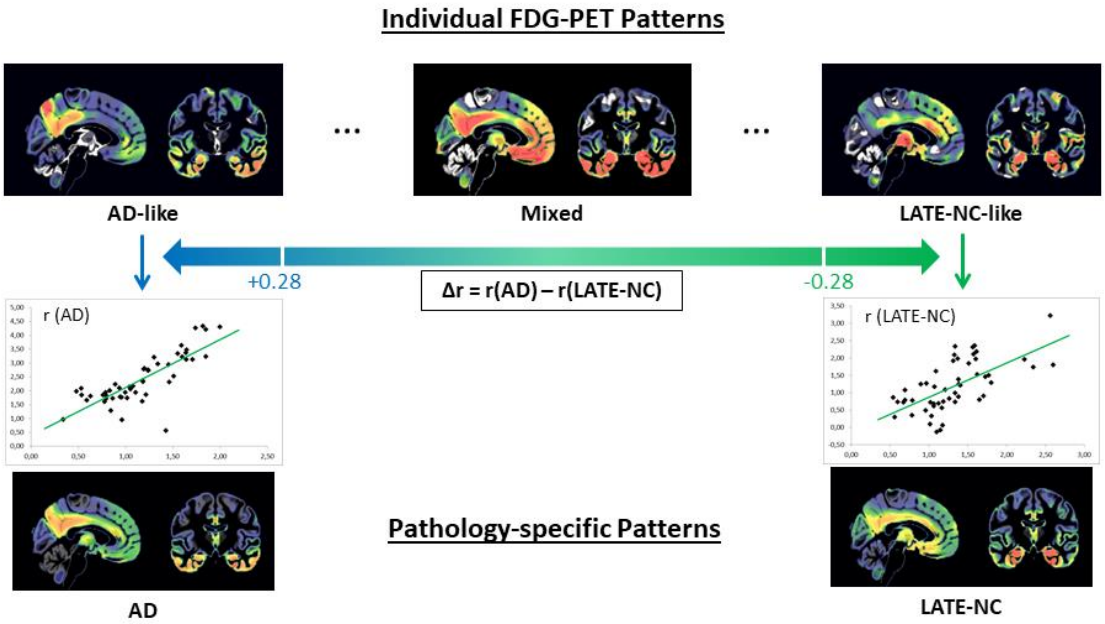

Schematic illustration of the pattern matching approach for classifying individual FDG-PET patterns according to the pathology-specific patterns. Individual hypometabolic patterns (FDG-PET SUVR Z-score maps, top) were assessed for their correspondence with the autopsy-based patterns of AD- and LATE-NC-typical hypometabolism (bottom) using spatial correlation. In the respective scatterplots (middle) each point corresponds to one of 52 cortical and subcorical brain regions defined in the Harvard-Oxford structural atlas. Patients showing a significant correspondence (i.e. $r>0.28$, corresponding to $p<0.05$) to any of the two patterns were then ordered along a continuum from most AD-like to most LATE-NC-like hypometabolism, which was quantified using the delta score between the respective spatial correlation coefficients ($\Delta r = r(AD) – r(LATE\text{-}NC)$). Patients were classified as „LATE-NC-like“ or „AD-like“ by applying a cutoff of $|\Delta r| > 0.28$ to the upper and lower parts of this distribution.

Supplementary Figure S3. Illustration of an alternative stratification approach based on a Gaussian Mixture Model analysis of the Δr distribution

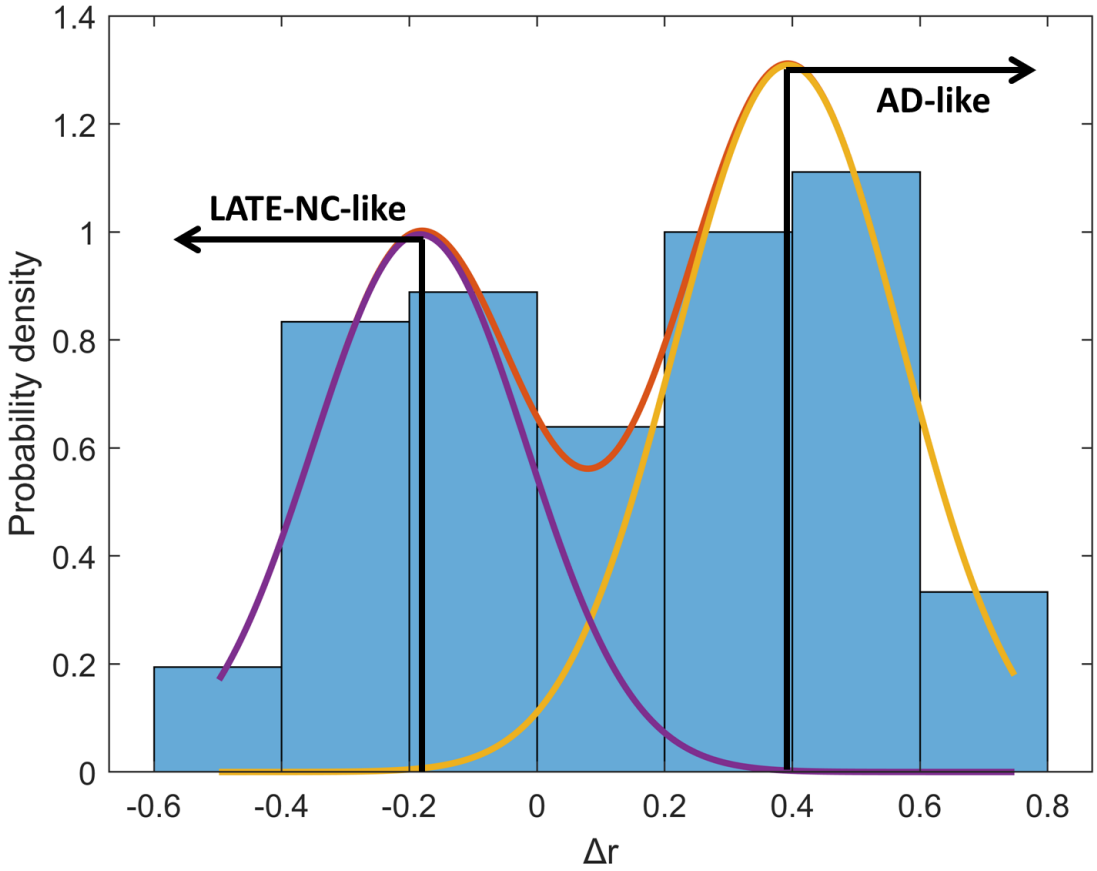

Gaussian Mixture Model (GMM) analysis of the Δr distribution revealed a bimodal distribution with an intersection close to Δr=0, though with a slight shift towards positive values. Classifying the negative and positive sides from the peaks of the respective distributions as (clearly) LATE-NC- and AD-like, respectively, resulted in a classification of 15 more patients as LATE-NC-like (Δr < -0.18 instead of -0.28) and 23 less patients as AD-like (Δr > 0.37 instead of 0.28). Characteristics of these patient groups are summarized in supplementary Table S2 below.

Supplementary Figure S4. Individual FDG-PET profiles of the two cases with hippocampal sclerosis in the comorbid AD+LATE-NC group

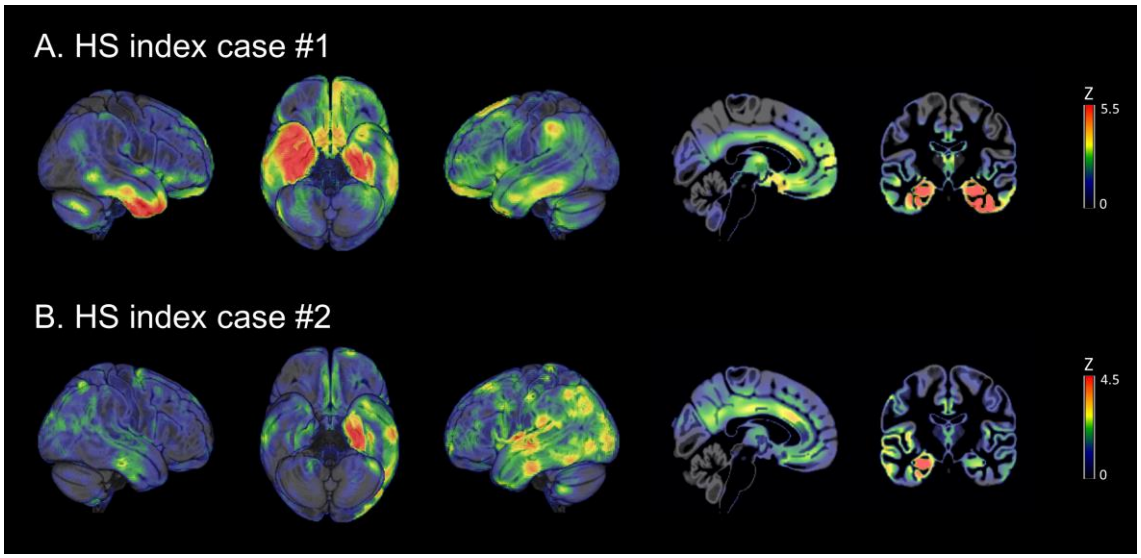

Figure shows individual Z-score maps of the two index cases with hippocampal sclerosis (HS) in the pathologic group with comorbid AD and LATE-NC. Color bars are scaled to the individual's peak Z-score. The visual resemblance with the LATE-NC-typical FDG-PET pattern is confirmed in both cases by a high spatial correlation coefficient (r(LATE-NC) = 0.88 and 0.58, for #1 and #2 respectively). Spatial correlation with the AD-typical pattern was lower at r(AD) = 0.59 and 0.31, respectively, resulting in automated classifications as LATE-NC-like patterns (Δr = -0.30 for #1 and -0.28 for #2).

Supplementary Figure S5. FDG-PET patterns of the stratified atypical and non-hypometabolic patient groups in the in-vivo cohort

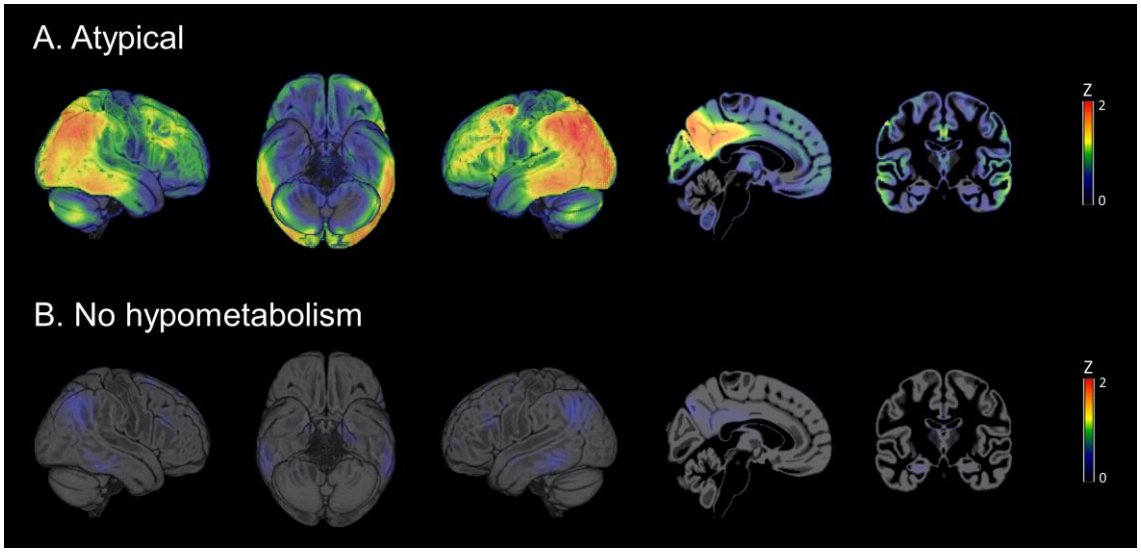

Figure shows average Z-score maps of clinically diagnosed AD dementia patients from the in-vivo cohort that exhibited atypical regional features (A) or lacked evidence of hypometabolism in any of the relevant areas (B). Note that average Z-scores are equivalent to Glass' Δ effect size.

Supplementary Figure S6. Group-specific trajectories of longitudinal cognitive decline

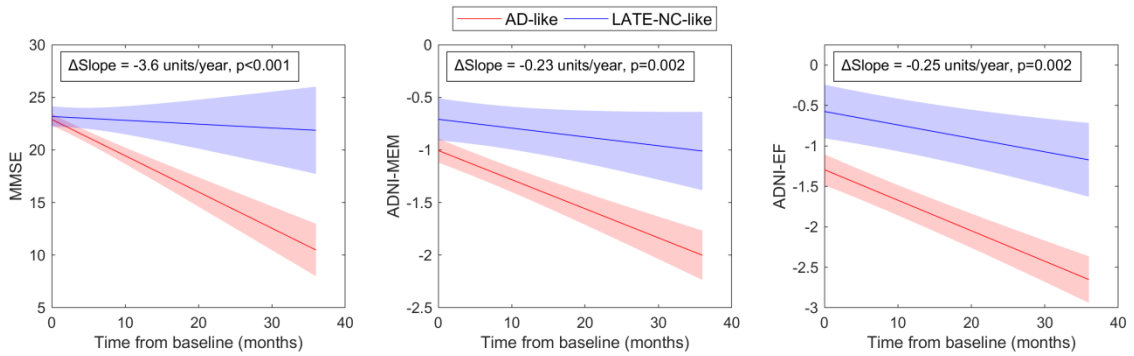

Cognitive trajectories of clinically diagnosed AD dementia patients with a LATE-NC-like (blue) or AD-like (red) hypometabolic pattern on FDG-PET. Cognitive assessments included MMSE scores for global cognitive functioning as well as domain-specific composite scores for memory (ADNI-MEM) and executive function (ADNI-EF). Differences in slopes (ΔSlope) represent the difference in annual rates of cognitive change of LATE-NC-like patients compared to AD-like patients; reported p-values correspond to the group x time interaction term of the linear mixed models.

Supplementary Figure S7. Associations with LATE-NC- vs AD-like FDG-PET pattern expression on a continuous scale

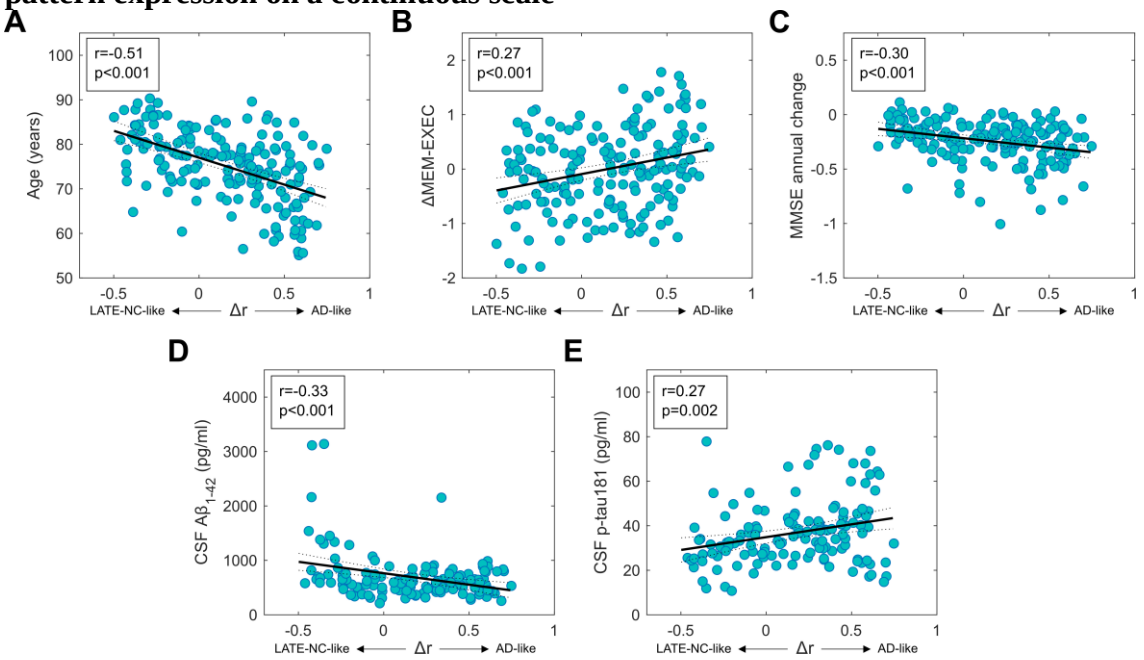

Associations of age (A), clinical features (B+C), and molecular biomarkers (D+E) with the hypometabolic pattern expression as a continuous variable (Δr). Reported r values represent Pearson correlation coefficients, together with the respective p-values. Solid black lines represent univariate regression lines and dotted lines represent 95% confidence bounds. Subject-specific annual rates of change in MMSE were estimated using both random and fixed effects from a linear mixed model.

Supplementary Figure S8. Individual hypometabolic profiles of LATE-NC cases

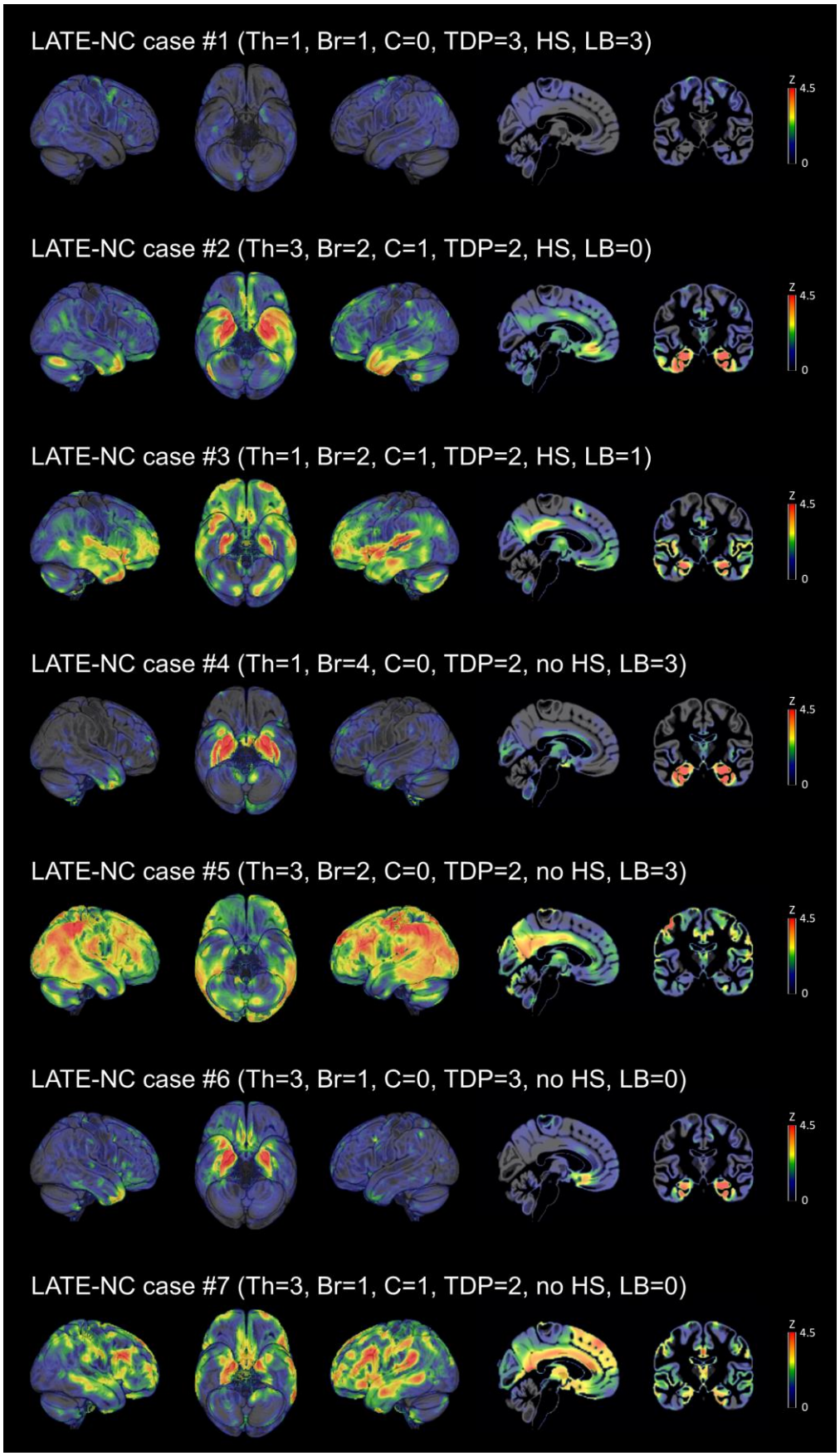

Th=Thal phase, Br=Braak stage, TDP=TDP-43 stage, HS=Hippocampal sclerosis, LB=Lewy body stage

Supplementary Figure S9. IMT ratio in relation to age

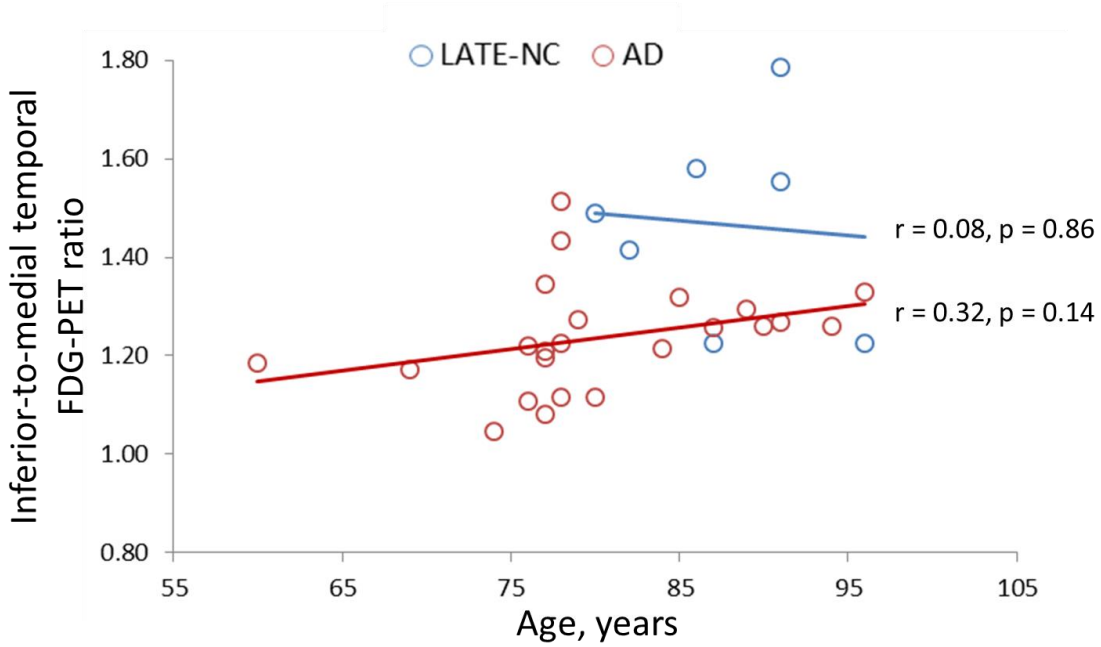

In order to examine whether a high inferior-to-medial temporal FDG-PET ratio may be associated with advanced age rather than LATE-NC, we plotted this ratio against age separately in the AD and LATE-NC groups. The AD group indeed showed a moderate positive association between age and the IMT ratio, though this did not reach statistical significance in this relatively small sample (r=0.32; p=0.14). However, the IMT ratio was still markedly higher in the LATE-NC cases compared to the AD cases in this elevated age range, and there was no relation between age and the IMT ratio in the LATE-NC group (r=0.08), indicating the relative specificity of this ratio for LATE-NC as compared to elevated age itself.

Supplementary Figure S10. FDG-PET pattern of age-matched AD group

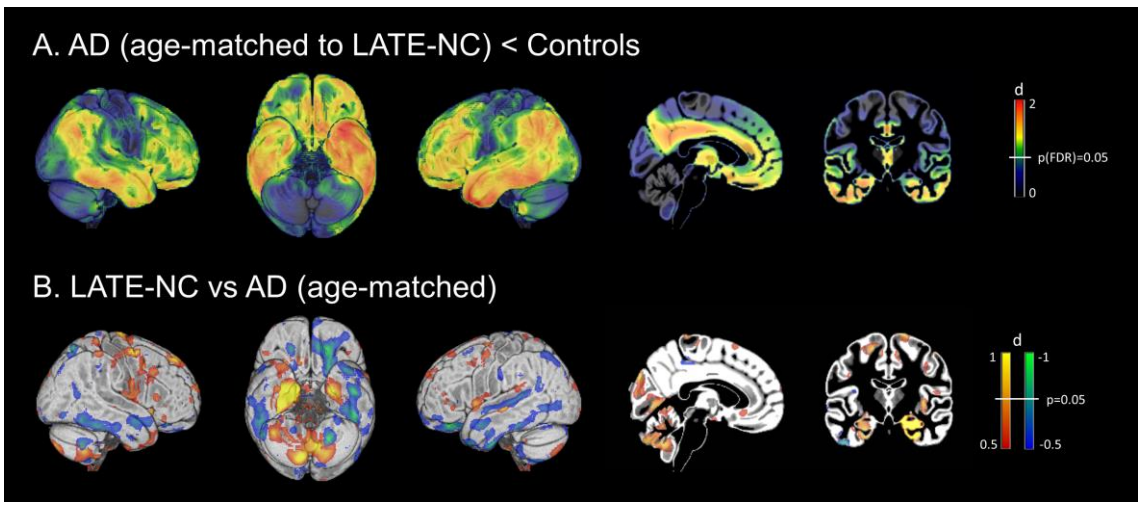

Illustration of the hypometabolic pattern of the subset of pathology-confirmed AD cases that were in the same age range as the LATE-NC cases (N=10; 80-96 years). A) Comparison to the cognitively normal control group (N=179). B) Direct comparison to

the LATE-NC group. Here, the blue-green color scale indicates more pronounced hypometabolism in AD and the red-yellow color scale indicates more pronounced hypometabolism in LATE-NC. Note how limiting the AD group to just the 10 cases in the same age range as the LATE-NC cases yielded a very similar "AD-typical" temporo-parietal FDG-PET pattern (with slightly more frontal involvement) compared to the whole AD group (displayed in Fig. 1 of the main manuscript; spatial correlation between these patterns: r = 0.88). Moreover, the effect size map for the direct contrast between LATE-NC and this age-matched AD group also showed very similar regional features as in the original comparison, including more pronounced medial temporal hypometabolism in LATE-NC and more pronounced inferior/lateral temporal hypometabolism in AD.

Supplementary Figure S11. LATE-NC-typical pattern using an age-matched control group

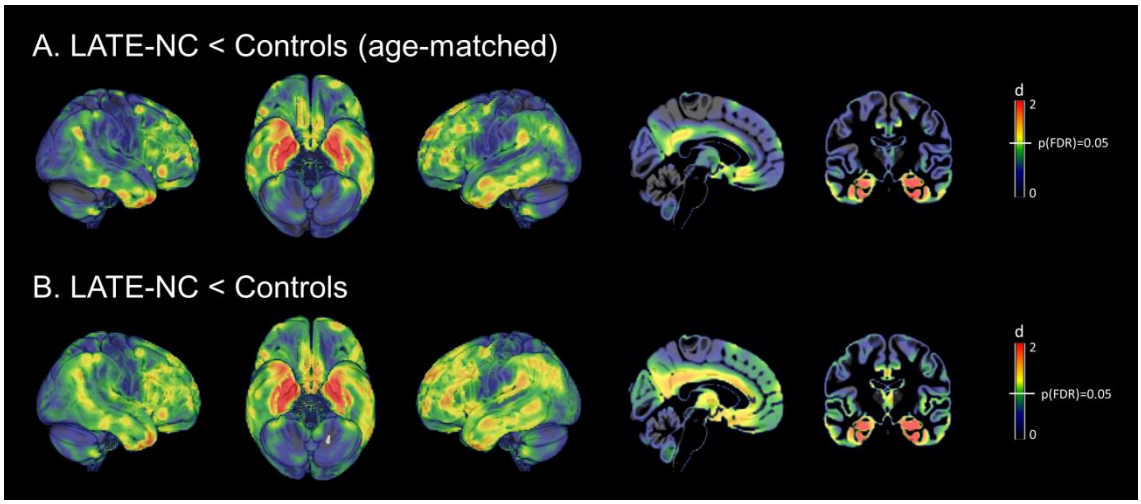

A) Illustration of the hypometabolic pattern of the LATE-NC group using an age-matched control group (≥ 80 years of age, N=38, range: 80-90 years, average: 83.3 ± 2.3 years). This analysis yielded a largely identical LATE-NC pattern (with slightly reduced effect sizes) as for the initial analysis (reproduced in (B)), with a spatial correlation between the two patterns of r = 0.97.

Supplementary Figure S12. FDG-PET patterns of pathologic groups without LATE-NC/AD and other pathologies

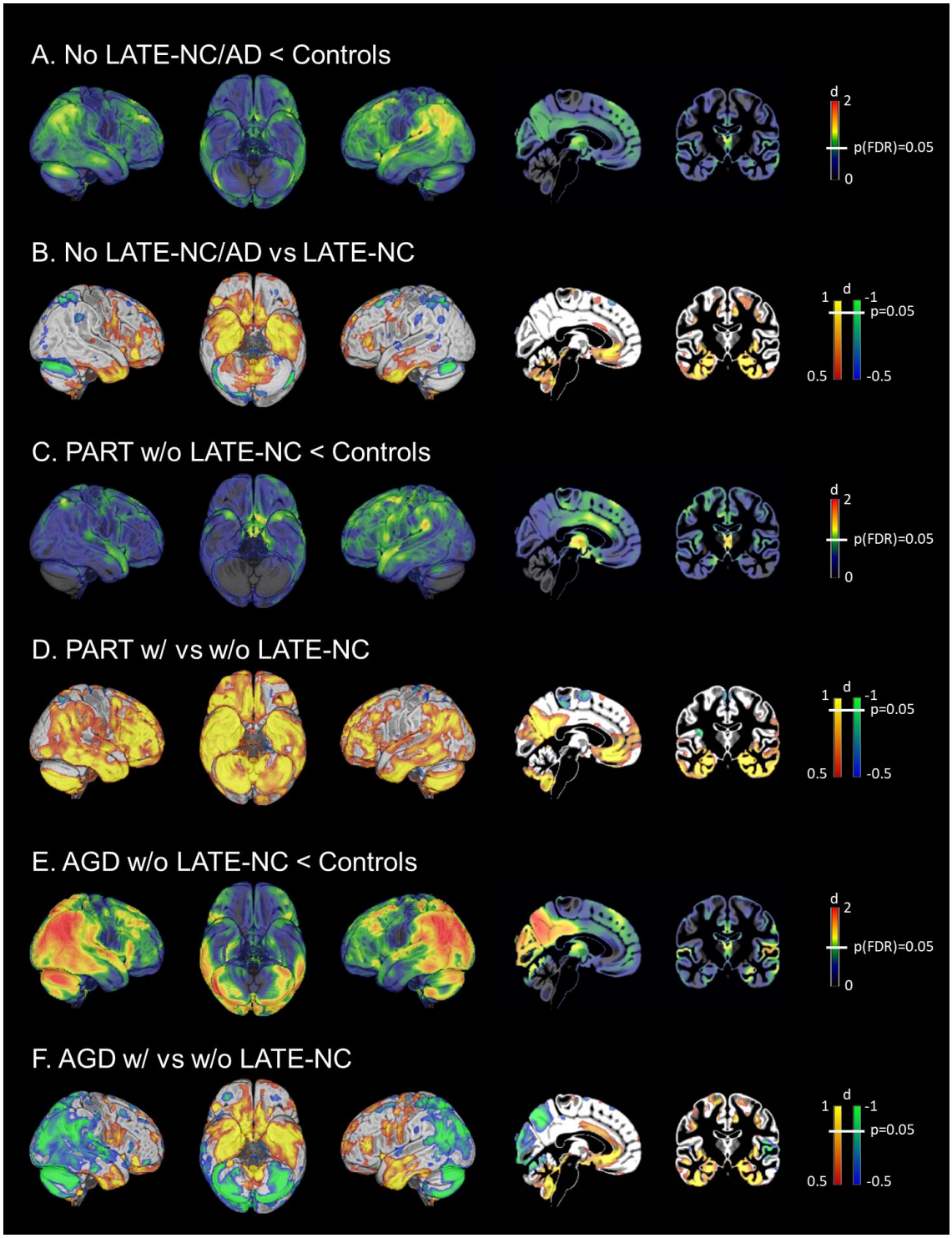

Hypometabolic patterns of different cognitively impaired non-AD pathologic groups compared to healthy controls and highest effect sizes compared to LATE-NC. (A, B) A mixed pathologic group defined by the absence of both LATE-NC and AD (ADNC≤1). (C, D) A group with primary age-related tauopathy (PART), defined as B score > 0, A score ≤ 2 and C score ≤ 1 [11], and no LATE-NC. (E, F) A group with argyrophilic grain disease (AGD) but no AD (ADNC≤1) or LATE-NC. AGD cases without LATE-NC are compared to AGD cases with LATE-NC.

Supplementary Table S1. Harvard-Oxford atlas ROIs used for screening for relevant hypometabolism

LATE-NC pattern relevant areas	AD pattern relevant areas
Hippocampus	Inferior_Temporal_Gyrus_anterior_division
Amygdala	Inferior_Temporal_Gyrus_posterior_division
Parahippocampal_Gyrus_anterior_division	Inferior_Temporal_Gyrus_temporooccipital_part
Parahippocampal_Gyrus_posterior_division	Supramarginal_Gyrus_anterior_division
Temporal_Pole	Supramarginal_Gyrus_posterior_division
Subcallosal_Cortex	Angular_Gyrus
Cingulate_Gyrus_anterior_division	Cingulate_Gyrus_posterior_division
Insular_Cortex	Precuneous_Cortex

Supplementary Table S2. Characteristics of LATE-NC-like and AD-like patient groups stratified according to a GMM-based approach

	Total Sample (N = 242)	LATE-NC-like (N = 40)	AD-like (N = 54)
Age (years)	74.9 ± 8.0	**81.1 ± 6.0**	**70.1 ± 8.5**
Sex (M/F)	143/99	25/15	18/26
Education (years)	15.3 ± 2.9	15.2 ± 2.9	15.9 ± 2.6
MMSE	23.2 ± 2.1	23.3 ± 2.0	23.0 ± 2.1
MEM	-0.89 ± 0.53	**-0.84 ± 0.45**	**-1.10 ± 0.53**
EXEC	-0.92 ± 0.93	**-0.67 ± 0.80**	**-1.37 ± 0.83**
Δ(MEM-EXEC)	0.03 ± 0.80	**-0.17 ± 0.76**	**0.28 ± 0.76**
CSF $A\beta_{42}$ (pg/ml)	704 ± 433	**1047 ± 715**	**599 ± 189**
CSF p-tau181 (pg/ml)	37 ± 16	**31 ± 14**	**41 ± 17**
APOE, 0/1/2 ε4 alleles, %pos	82/112/47, 66%	**21/18/1, 48%**	**21/22/11, 61%**
TMEM106B, 0/1/2 T alleles, % pos	36/105/69, 83%	3/19/13, 91%	8/27/14, 84%
GRN, 0/1/2 T alleles, % pos	104/80/26, 51%	16/12/7, 54%	17/27/5, 65%

Significant differences (at $p<0.05$) between LATE-NC-like and AD-like groups, as classified according to a Gaussian Mixture Model (GMM) analysis (illustrated in suppl. Fig. S3), are printed in bold; differences with trend-level statistical significance ($p<0.1$) are printed in italics.

N = Sample size, M = Male, F = Female, MEM = memory composite score, EXEC = executive function composite score

Supplementary Table S3. Characteristics of patients stratified according to the inferior-to-medial temporal metabolism ratio

	LATE-NC-like (above cutoff) (N = 48)	LATE-NC-like (upper extreme) (N=25)	AD-like (below cutoff) (N = 166)	AD-like (lower extreme) (N=77)
Age (years)	**80.0 ± 5.8**	**80.3 ± 5.9**	**73.9 ± 8.0**	**71.6 ± 8.3**
Sex (M/F)	31/17	18/7	98/68	41/36
Education (years)	15.6 ± 2.8	15.0 ± 3.3	15.2 ± 2.9	15.7 ± 2.4
MMSE	23.1 ± 2.0	22.6 ± 2.1	23.1 ± 2.1	23.0 ± 2.1
MEM	-0.88 ± 0.48	-0.93 ± 0.49	-0.96 ± 0.52	-1.06 ± 0.58
EXEC	*-0.80 ± 0.83*	**-0.82 ± 0.93**	*-1.07 ± 0.89*	**-1.30 ± 0.94**
Δ(MEM-EXEC)	-0.08 ± 0.80	*-0.12 ± 0.84*	0.10 ± 0.77	*0.23 ± 0.80*
CSF $A\beta_{42}$ (pg/ml)	**957 ± 688**	**968 ± 703**	**619 ± 268**	**631 ± 290**
CSF p-tau181 (pg/ml)	*33.5 ± 15.1*	32.5 ± 14.1	*37.6 ± 15.0*	37.8 ± 16.2
APOE, 0/1/2 ε4 alleles, % pos	18/24/6, 63%	10/13/2, 60%	55/78/33, 67%	33/32/12, 57%
TMEM106B, 0/1/2 T alleles, % pos	4/20/16, 90%	**2/10/11, 91%**	27/80/43, 82%	**12/41/14, 82%**
GRN, 0/1/2 T alleles, % pos	19/13/8, 53%	8/10/5, 65%	74/61/15, 51%	28/30/9, 58%

Patients were stratified using the inferior-to-medial temporal metabolism ratio in two different ways. First, all patients above the autopsy-derived inferior-to-medial temporal ratio cutoff (1.38) were classified as LATE-NC-like, all patients below that cut-off as AD-like. In a complementary stratification, only patients at the upper and lower parts of the inferior-to-medial temporal ratio distribution were classified as LATE-NC- and AD-like, respectively, and numbers in each group were matched to the pattern-matched LATE-NC- and AD-like groups (i.e., the 25 patients with the highest inferior-to-medial temporal ratio were classified as LATE-NC-like, and the 77 patients with the lowest ratio as AD-like).

Significant differences (at $p<0.05$) between LATE-NC-like and the respective AD-like comparison group are printed in bold, differences with trend-level statistical significance ($p<0.1$) are printed in italics.

N = Sample size, M = Male, F = Female, MEM = memory composite score, EXEC = executive function composite score

Supplementary Table S4. Contingency table of group assignments based on pattern matching compared to the inferior-to-medial temporal ratio

	Above IMT cutoff (N=48)	Below IMT cutoff (N=166)	Upper IMT extreme (N=25)	Lower IMT extreme (N=77)
LATE-NC-like (N=25)	23	2	18	0
AD-like (N=77)	0	77	0	55
Mixed (N=78)	21	57	7	7
Atypical (N=34)	4	30	0	15

Twenty-three of the 25 patients that had been classified as LATE-NC-like by the pattern matching approach also fell above the Inferior-to-medial temporal (IMT) cutoff indicative of LATE-NC (>1.38), and one additional pattern-matched LATE-NC-like case lay just below this cutoff (1.37). Of the remaining 25 subjects with IMT ratio values above the cutoff, 21 had been classified as a mixed profile by the pattern matching approach and 4 as not matching any of the two pathology-specific patterns. None of the patients above the IMT cutoff had been classified as AD-like by the pattern matching approach. When considering the number-matched upper and lower parts of the IMT ratio, 18 of the 25 patients with highest IMT ratios had also been classified as LATE-NC-like by the pattern matching approach (72%), and the other 7 patients (28%) had been classified as a mixed profile. Similarly, 55 of the 77 patients with lowest IMT ratios had also been classified as AD-like by the pattern matching approach (71%), whereas 15 (19%) had been classified as atypical and only 7 (9%) as showing a mixed profile.

References

[1] Franklin EE, Perrin RJ, Vincent B, Baxter M, Morris JC, Cairns NJ. Brain collection, standardized neuropathologic assessment, and comorbidity in Alzheimer's Disease Neuroimaging Initiative 2 participants. Alzheimer's & dementia : the journal of the Alzheimer's Association. 2015;11:815-22.

[2] Katsumata Y, Fardo DW, Kukull WA, Nelson PT. Dichotomous scoring of TDP-43 proteinopathy from specific brain regions in 27 academic research centers: associations with Alzheimer's disease and cerebrovascular disease pathologies. Acta neuropathologica communications. 2018;6:142.

[3] Nelson PT, Dickson DW, Trojanowski JQ, Jack CR, Boyle PA, Arfanakis K, et al. Limbic-predominant age-related TDP-43 encephalopathy (LATE): consensus working group report. Brain : a journal of neurology. 2019.

[4] Crane PK, Carle A, Gibbons LE, Insel P, Mackin RS, Gross A, et al. Development and assessment of a composite score for memory in the Alzheimer's Disease Neuroimaging Initiative (ADNI). Brain imaging and behavior. 2012;6:502-16.

[5] Gibbons LE, Carle AC, Mackin RS, Harvey D, Mukherjee S, Insel P, et al. A composite score for executive functioning, validated in Alzheimer's Disease Neuroimaging Initiative (ADNI) participants with baseline mild cognitive impairment. Brain imaging and behavior. 2012;6:517-27.

[6] Levin F, Ferreira D, Lange C, Dyrba M, Westman E, Buchert R, et al. Data-driven FDG-PET subtypes of Alzheimer's disease-related neurodegeneration. Alzheimer's research & therapy. 2021;13:49.

[7] Risacher SL, Anderson WH, Charil A, Castelluccio PF, Shcherbinin S, Saykin AJ, et al. Alzheimer disease brain atrophy subtypes are associated with cognition and rate of decline. Neurology. 2017;89:2176-86.

[8] Murray ME, Cannon A, Graff-Radford NR, Liesinger AM, Rutherford NJ, Ross OA, et al. Differential clinicopathologic and genetic features of late-onset amnestic dementias. Acta neuropathologica. 2014;128:411-21.

[9] Josephs KA, Whitwell JL, Tosakulwong N, Weigand SD, Murray ME, Liesinger AM, et al. TAR DNA-binding protein 43 and pathological subtype of Alzheimer's disease impact clinical features. Annals of neurology. 2015;78:697-709.

[10] Josephs KA, Murray ME, Tosakulwong N, Weigand SD, Knopman DS, Petersen RC, et al. Brain atrophy in primary age-related tauopathy is linked to transactive response DNA-binding protein of 43 kDa. Alzheimer's & dementia : the journal of the Alzheimer's Association. 2019.

[11] Crary JF, Trojanowski JQ, Schneider JA, Abisambra JF, Abner EL, Alafuzoff I, et al. Primary age-related tauopathy (PART): a common pathology associated with human aging. Acta neuropathologica. 2014;128:755-66.

[12] Arnold SJ, Dugger BN, Beach TG. TDP-43 deposition in prospectively followed, cognitively normal elderly individuals: correlation with argyrophilic grains but not other concomitant pathologies. Acta neuropathologica. 2013;126:51-7.

[13] Jicha GA, Nelson PT. Hippocampal Sclerosis, Argyrophilic Grain Disease, and Primary Age-Related Tauopathy. Continuum (Minneapolis, Minn). 2019;25:208-33.

[14] Murray ME, Graff-Radford NR, Ross OA, Petersen RC, Duara R, Dickson DW. Neuropathologically defined subtypes of Alzheimer's disease with distinct clinical characteristics: a retrospective study. The Lancet Neurology. 2011;10:785-96.

[15] Ferreira D, Nordberg A, Westman E. Biological subtypes of Alzheimer disease: A systematic review and meta-analysis. Neurology. 2020;94:436-48.

[16] Whitwell JL, Dickson DW, Murray ME, Weigand SD, Tosakulwong N, Senjem ML, et al. Neuroimaging correlates of pathologically defined subtypes of Alzheimer's disease: a case-control study. The Lancet Neurology. 2012;11:868-77.